A&A 489, 281–289 (2008)
DOI: 10.1051/0004-6361:20078530

Astronomy & Astrophysics

Pulsar kicks by anisotropic neutrino emission from quark matter in strong magnetic fields

I. Sagert and J. Schaffner-Bielich

Institute for Theoretical Physics/Astrophysics, Goethe University, Max-von-Laue-Straße 1, 60438 Frankfurt, Germany
e-mail: sagert@th.physik.uni-frankfurt.de

Received 22 August 2007 / Accepted 24 May 2008

ABSTRACT

Aims. We critically discuss a pulsar acceleration mechanism based on asymmetric neutrino emission from the direct quark Urca process in the interior of proto neutron stars.
Methods. The neutrinos are emitted by the cooling strange quark matter core with an anisotropy caused by a strong magnetic field. We calculate the kick velocity of the proto neutron star in dependence of the temperature and radius of the quark phase. The results are compared with the necessary magnetic field strength, as well as the neutrino mean free path.
Results. We find that within a quark phase radius of 10 km and temperatures higher than 5 MeV kick velocities of 1000 km s^{-1} can be reached only when neutrino quark scattering is ignored. When taking the neutrino mean free paths in quark matter into account kick velocities higher than 100 km s^{-1} cannot be reached. The same holds even when effects from colour superconductivity are included. For pulsar kicks powered by quark phase transitions from an ungapped quark phase to the CFL phase the final velocity depends crucially on the pairing gap and the quark chemical potential and reaches 1000 km s^{-1} only in marginal cases.
Conclusions. We find that the phenomenon of pulsar kick velocities higher than 100 km s^{-1} cannot be explained by asymmetric neutrino emission from either cooling normal strange quark or colour superconducting quark matter due to the small neutrino mean free paths. If neutrinos are produced by a phase transition to colour-superconducting quark matter, high kick velocities can only be reached for temperatures below 1 MeV.

Key words. dense matter – stars: magnetic fields – stars: neutron – neutrinos – pulsars: general

1. Introduction

1.1. Pulsar kicks

Proper motion measurements of pulsars imply a transverse velocity spectrum ranging up to ≥1000 km s^{-1} (see Hobbs et al. 2005; Cordes & Chernoff 1998; Chatterjee et al. 2005). Both the initial proper motion distribution and the origin of these high velocities are still under discussion. The former can be fit both by a single Maxwellian distribution with a mean velocity of 400 km s^{-1} (Hobbs et al. 2005) and by a two-component velocity distribution with characteristic velocities of 90 km s^{-1} and 500 km s^{-1} (Arzoumanian et al. 2002), whereas Bombaci & Popov (2004) propose that the latter can be explained by the simultaneous existence of neutron stars and quark stars. The general assumption for explaining the high velocities is that, during a certain time period in their evolution, neutron stars experience an accelerating kick, a so-called pulsar kick. This could be induced by a hydrodynamic mechanism (Burrows et al. 2006; Janka et al. 2007), based on an asymmetric supernova explosion, disruption of binary systems (Gott et al. 1970) or asymmetric low-frequency electromagnetic radiation due to an off-centred rotating dipole (Harrison & Tademaru 1975; for an overview see e.g. Wang et al. 2006; Lai et al. 2001). Another widely discussed class of acceleration mechanisms for pulsars is based on asymmetric neutrino emission (Dorofeev et al. 1985).

1.2. Pulsar acceleration by asymmetric neutrino emission

When assuming an energy release in neutrinos of around ∼10^{53} erg during a supernova one gets from momentum conservation that an asymmetry of about 3% could accelerate a neutron star of 1.4 $M_\odot$ to velocities of 1000 km s^{-1}. Strong magnetic fields coupled with parity violation in weak interaction can induce anisotropies in the neutrino-momentum distribution. In connection to this, it is interesting to note that comparisons of spin orientations with axes of proper motion via fitting pulsar wind tori (Ng & Romani 2004) showed a good alignment between the velocity vector and the rotational axis for the Crab, as well as the Vela pulsar (Brisken et al. 2005). Similarly, strong indications for such an alignment could be seen for the case of 25 pulsars as shown by Johnston et al. (2005). Recently, Ng & Romani (2007) have explored the correlation between pulsar spin and proper motion assuming a single acceleration kick during the proto neutron star cooling and find that the thrust scaled proportionally to the neutrino luminosity. The preferred fit parameters are consistent with a magnetic field induced asymmetry of a neutrino driven kick where the characteristic timescales for the anisotropic emission are 1–3 s. Similar conclusions were derived by Wang et al. (2006).

The scenario of neutrino driven kicks has been examined by Horowitz & Piekarewicz (1998) for the capture of polarised electrons in proto neutron stars. The required magnetic fields were found to be ∼10^{16} Gauss throughout the star. For lower magnetic fields, Horowitz & Li (1998) studied cumulative parity violation in neutrino elastic scattering from polarised neutrinos. It was shown then by Kusenko et al. (1998) that no asymmetry would be generated in thermal equilibrium for such processes even in the presence of anisotropic scattering amplitudes (known as "no-go theorem"). However, the neutrino transport properties and emissivities change in the presence of exotic matter and can

influence this scenario. Consequently, in this work we investigate a neutrino kick mechanism for proto-neutron stars with neutrinos stemming from a cooling quark matter core.

1.3. Quark matter in compact stars

Quark matter is expected to appear if the density inside the neutron star exceeds 2–3 times normal nuclear density (Glendenning 1992). This can take place very soon after the formation of the neutron star in the supernova explosion, during the proto-neutron star cooling stage, or it can be delayed on timescales of the order of days or years depending on the mass of the metastable star (see Drago et al. 2004, and references therein). For quark stars, one distinguishes between hybrid stars and strange or selfbound stars. For the former, quark matter can be present in a mixed phase with hadrons or form a pure quark matter core (Schertler et al. 2000; Glendenning & Kettner 2000). If strange quark matter is absolutely stable, it can form selfbound stars completely made of strange quark matter only covered by a thin hadronic or strangelet crust. The first pure quark star was calculated by Itoh (1970) followed up today by a large sample of approaches for quark matter (for an overview see Schaffner-Bielich 2007, 2005; Weber 2005). Up to now, quark stars cannot be excluded by observation, because they are even compatible with pulsar masses up to two solar masses, as pointed out by Alford et al. (2007).

One of the approaches to quark matter in the interior of compact stars is colour-superconductivity, where quarks form Cooper pairs with a net colour charge (Barrois 1977; Bailin & Love 1984; Rapp et al. 1998; Alford et al. 1998; for overviews of colour-superconductivity see e.g. Huang 2005; Alford 2001; Shovkovy 2005; Rischke 2004; Rajagopal & Wilczek 2000). Depending on the temperature and the baryon chemical potential up, down, and strange quarks participate differently in the pairing. However, for the highest densities with quark chemical potential greater than 400 MeV the up, down, and strange quarks of all colours form Cooper pairs. This case is called the colour-flavour locked (CFL) phase (Alford et al. 1999; Rapp et al. 2000). Due to the required quark chemical potentials of $\mu_q > 300$ MeV and temperatures of $T < 100$ MeV (Rüster et al. 2005) it is assumed that colour superconductivity is realized in the interior of strange and hybrid stars.

Sandin & Blaschke (2007) study newborn proto-neutron stars and find that their cores are in the 2SC state and that stable quark star solutions with CFL cores exist only at low temperatures and neutrino chemical potentials. Stable solutions for a CFL core have also been obtained by Pagliara & Schaffner-Bielich (2008); furthermore, the authors find stable hybrid stars configurations with a 2SC layer and a CFL core. During the past years, there have been different approaches to explaining pulsar kicks in connection with colour-superconducting quark matter (Schmitt et al. 2005; Berdermann et al. 2006) assuming asymmetric gap functions in a spin-1 colour superconducting core and beaming of neutrino emission along magnetic vortex lines embedded in CFL quark matter, respectively.

1.4. Pulsar kicks by anisotropic neutrino emission from quark matter

Studying asymmetric neutrino emission from the direct quark Urca process in a strong magnetic field also leads to a new problem not present for nucleon Urca processes. For quark matter, the axial and vector coupling constants are equal, and simply applying the result of Horowitz & Piekarewicz (1998) would give a vanishing neutrino asymmetry. In the centre of mass reference frame the neutrino production from electron capture by up quarks is isotropic. Only left handed particles take part in this process. In the presence of a strong magnetic field, the electron spin is polarised opposite to the magnetic field direction. In the rest frame of the star the quarks have momenta in the range of 400 MeV, whereas the electron momentum is less than 100 MeV. In the boosted frame, the momenta of the scattered particles are beamed in the direction of the incident particle (Byckling & Kajantie 1973). The momenta of the down quark and the neutrino are beamed in the direction of the up quark momentum, creating a "neutrino emission cone". Positron capture in the centre of mass reference frame creates an "antineutrino cone" in the same direction. Consequently we expect a polarised neutrino emission along the magnetic axis opposite the field direction. For simplicity we assume that the angle ϕ between the magnetic field axis and the rotational axis is small as found by Ng & Romani (2007).

The aim of this paper is to critically examine this acceleration mechanism for cooling proto neutron stars containing a strange quark matter core. The discussion will be based on energy arguments comparing the required magnetic field strengths with the energy release for the acceleration and the neutrino mean free path in the compact star. We do not discuss here the influence of the magnetic field on the equation of state nor include hydrodynamic or hydrostatic aspects of the quark core in our analysis. However, as any refined discussion should fulfil the basic constraints on temperature, magnetic field, and neutrino mean free path we set here, this analysis can serve as a starting point for more advanced studies.

The paper is organised as follows. In the next section we will discuss estimates for the degree of electron spin polarisations depending on temperature, electron chemical potential and magnetic field strength. For a sufficient acceleration the energy stored in the proto neutron star matter must equal the kinetic energy of a pulsar kick. Hence, in Sect. 3 we use the energy density and heat capacity of quark matter and electrons to calculate the kick velocities analytically and numerically for polarised electrons. In Sect. 4 we then discuss the interplay between the neutrino mean free paths and the acceleration mechanism. Finally, in Sect. 5 we comment on the acceleration mechanism for strange stars in the CFL phase, and pulsar kicks by quark matter phase transitions and close with a summary and an outlook.

2. Polarisation

Electrons that are moving in a magnetic field larger than $B_{\rm crit} \sim 4.4 \times 10^{13}$ Gauss are situated in Landau levels perpendicular to the magnetic field axis. Their energy is quantised and can be written as (Shul'man 2001):

$$E^2 = {m_{\rm e}}^2 + {p_z}^2 + 2eB\eta = {m_{\rm e}}^2 + {p_z}^2 + eB[(2\nu + 1) \mp 1], \qquad (1)$$

where the last term in Eq. (1) corresponds to the kinetic energy in the plane. The magnetic field B is pointing in the positive z-direction. The Landau level number η is defined by its quantum number ν and the electron spin s as:

$$\eta = \nu + \frac{1}{2} + s \text{ and } s = \begin{cases} +\frac{1}{2} & \text{for } n_+ \\ -\frac{1}{2} & \text{for } n_-. \end{cases} \qquad (2)$$

The electron number densities n_+ and n_- in Eq. (2) denote electrons with spin parallel or anti-parallel to the magnetic field

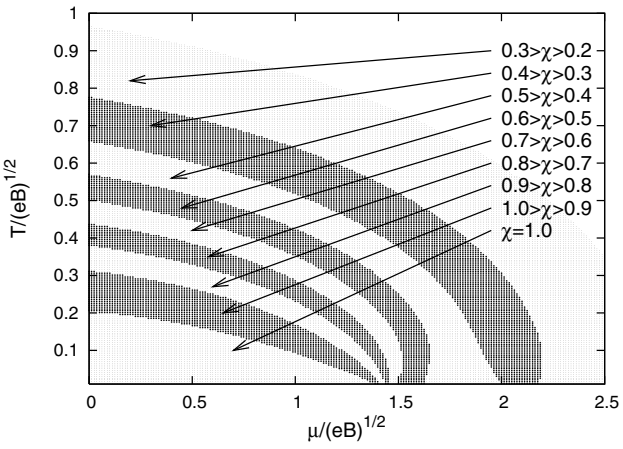

Fig. 1. Spin polarisation for temperature and electron chemical potential scaled by the magnetic field.

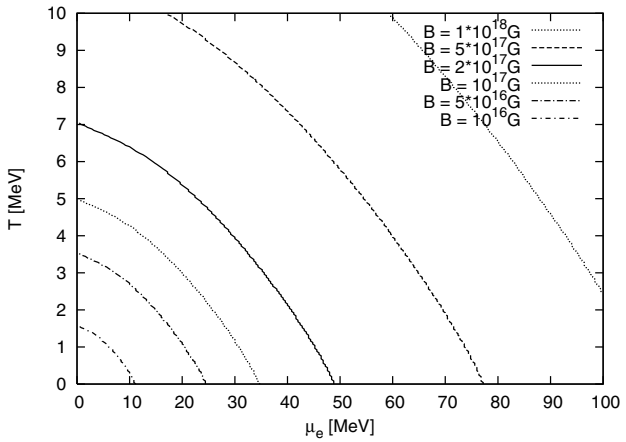

Fig. 2. Constraint to fully polarise the electron spin for different magnetic fields in dependence on the temperature and the electron chemical potential.

direction, respectively:

$$n_{\mp} = \frac{geB}{(2\pi)^2}\int_{\eta_{\min\mp}}^{\eta_{\max}}\int_0^{\infty} f(E)\mathrm{d}\eta\mathrm{d}p_z = \frac{geB}{(2\pi)^2}\sum_{\eta_{\min\mp}}^{\eta_{\max}}\int_0^{\infty} f(E)\mathrm{d}p_z \quad (3)$$

with the degeneracy factor g, the Fermi distribution function

$$f(E) = \left(\exp\left((E-\mu_e)/T\right)+1\right)^{-1}, \quad (4)$$

and the energy E given by Eq. (1). For a sufficiently high magnetic field, all electrons are situated in the lowest Landau level with $\eta = 0$ and spin $s = -1/2$.

In the following we discuss the dependence of the electron spin polarisation

$$\chi = (n_- - n_+)\,/\,(n_- + n_+) \quad (5)$$

on temperature, electron chemical potential, and magnetic field. Figure 1 shows the polarisation depending on T and μ_e, where both are scaled by the magnetic field. It is assumed that the energy range is much higher than the electron mass so that it can be neglected. A growing temperature and chemical potential decrease the spin polarisation. Such behaviour is expected, since the additional energy helps the electrons to overcome the energy gap of $\sqrt{2eB}$ to the next higher Landau level. Figure 2 shows the constraints on the temperature and the electron chemical potential to fully polarise the electron spin, which is $\chi = 1$, in dependence of the magnetic field. The temperatures range up to 10 MeV and μ_e up to 100 MeV. The required magnetic fields are found to be quite strong, between 10^{16} G and 10^{18} G. Although they lie below the critical value of $\sim 1.3 \times 10^{18}$ Gauss for the stability of a magnetised neutron stars (Lai & Shapiro 1991), magnetic field strengths of $B \geq 10^{17}$ G are not observed for compact stars. However, here high magnetic fields are required to be present in the quark phase and can decrease towards the surface of the star.

We calculated the polarisation for four different cases: vanishing temperature ($T = 0$), both the non-degenerate massless ($\mu, m \ll \sqrt{2eB} \ll T$) and the non-degenerate massive cases ($\mu = 0, m \gg T \gg \sqrt{2eB}$), and finally for large magnetic fields with non-vanishing temperature ($\mu, m, T \ll \sqrt{2eB}$). The results are summarised in Table 1.

The assumption of zero temperature is usually adopted for describing cold compact stars. The number of Landau levels is limited to $\eta_{\max} = (\mu^2 - m^2)/(2eB)$ where μ is the electron chemical potential. For $E = \mu$, the electron number densities $n_{\mp}$ become

$$n_{\mp} = \frac{eB}{(2\pi)^2}\sum_{\nu=0/1}^{(\mu^2-m^2)/(2eB)} \sqrt{\mu^2 - m^2 - 2\nu eB}. \quad (6)$$

This relation for the polarisation is easy to understand since an increase of the chemical potential transfers energy to the electrons. Hence, they can overcome the energy gap of $\sqrt{2eB}$ to a new Landau level with $\eta > 0$ where both spin directions are possible, which decreases the value for the spin polarisation χ. A look at Fig. 3a, where the analytical and numerical results are plotted, shows very good agreement between these two approaches. The steps that appear in the polarisation curve correspond to the opening of the next Landau level. For sufficiently high chemical potentials, the number of Landau levels becomes so high that the effects from the energy quantisation become negligible and the steps disappear.

The non degenerate, massless case ($\mu, m \ll \sqrt{2eB} \ll T$) describes hot proto-neutron stars where temperatures of more than 50 MeV (Lattimer & Prakash 2004) can be present. Hence, $\sqrt{2eB} \lesssim T$ holds for magnetic fields $B \leq 10^{17}$ G. The electron mass and chemical potential can be assumed to be negligible. As $\sqrt{2eB} \ll T$ the number of Landau levels will be very high so we can again replace the summation over η in Eq. (4) by an integration. With $\mu, m \ll \sqrt{2eB}$ we get

$$\begin{aligned} n_- &= \frac{eB}{(2\pi)^2}\int \mathrm{d}p \int_0^{\infty} \mathrm{d}\eta \frac{1}{\mathrm{e}^{\sqrt{p^2+2\eta eB}/T}+1} = \frac{3\zeta(3)T^3}{8\pi^2}, \\ n_+ &= \frac{3\zeta(3)T^3}{8\pi^2} - \frac{eB}{4\pi^2}T\ln(2), \end{aligned} \quad (7)$$

where $\zeta(x)$ is the Zeta-function. From Table 1 we see that, for an electron gas with $\mu, m \ll \sqrt{2eB} \ll T$, the polarisation χ is proportional to eB/T^2. The higher the temperature, the more Landau levels are accessible for the electrons, and the electron spin polarisation decreases.

A star where the electron mass m can be assumed to be higher than the temperature and the magnetic field could be an old quark star with a colour-superconducting quark phase where the electron chemical potential is vanishingly small (e.g. quark matter in the CFL phase). The electron number densities can be

Table 1. Summary of analytic solutions for the polarisation as discussed in Sect. 2.

Polarisation χ for	General expression for χ	Approximation for χ
$T = 0$	$\left(2\sum_{\nu=1}^{\frac{\mu_e^2-m^2}{2eB}}\sqrt{1-\frac{2\nu eB}{\mu_e^2-m^2}}+1\right)^{-1}$	$3eB/(2\mu_e^2)$ for $\mu_e \gg \sqrt{2eB}, m$
$T \gg 2eB \gg \mu, m$	$\left(3\frac{T^2}{eB}\frac{\zeta(3)}{\ln 2}-1\right)^{-1}$	$eB\ln 2/(3\zeta(3)T^2)$ as $T^2 \gg 2eB$
$m \gg T \gg 2eB, \mu_e = 0$	$\left(\frac{2T}{eB}\frac{mK_0[m/T]+TK_1[m/T]}{K_1[m/T]}-1\right)^{-1}$	$eB/(2mT)$ for $m \gg T$
$2eB \gg T \gg m, \mu$	$\left(1+\frac{4}{\ln(2)}\sqrt{\frac{\pi T}{4eB}}\exp(-\sqrt{2eB}/T)\right)^{-1}$	...

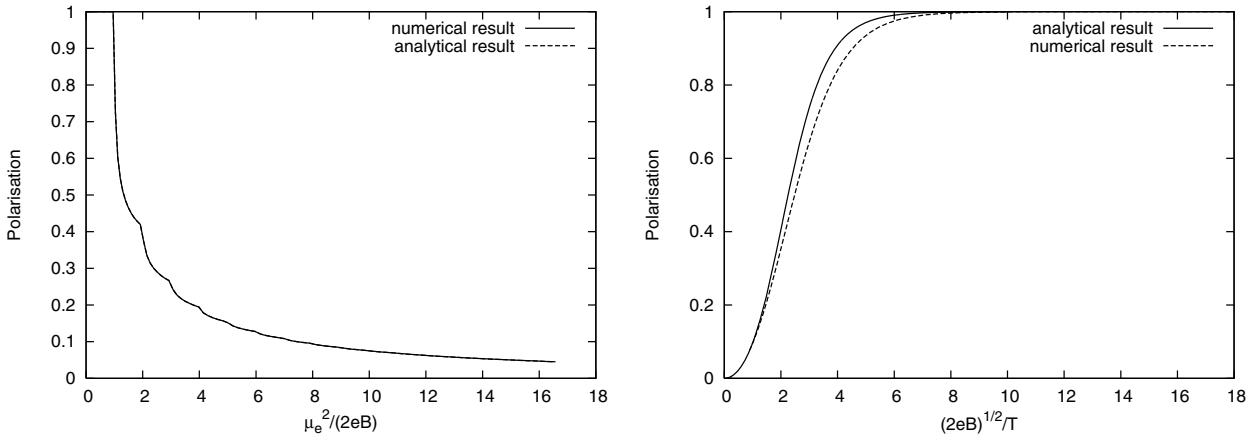

Fig. 3. Comparison of the numerical and analytical results for the electron spin polarisation. **a)** gives the polarisation for $T = 0$ and **b)** shows the case of $\mu, m \ll T \ll \sqrt{2eB}$. The difference between the numerical and the analytical results in the latter is max. 10%.

derived by applying the Taylor-expansion for small $x = 2eB/T^2$ and replacing the summation for weak fields again with an integration over η:

$$n_- \simeq \frac{eB}{(2\pi)^2}\int \mathrm{d}p \int_0^\infty \mathrm{d}\eta \frac{1}{\exp\left(\frac{\sqrt{p^2+m^2}}{T}+\frac{\eta eB}{\sqrt{p^2+m^2}T}\right)+1} \quad (8)$$

$$\simeq \frac{T}{(2\pi)^2}\left(m^2K_0\left[m/T\right]+mTK_1\left[m/T\right]\right), \quad (9)$$

$$n_+ = \frac{T}{(2\pi)^2}\left(m^2K_0\left[m/T\right]+mTK_1\left[m/T\right]\right) - \frac{eBm}{(2\pi)^2}K_1\left[m/T\right]. \quad (10)$$

Here, K_1 and K_0 are the modified Bessel functions of the second kind.

For the magnetic field strength much larger than the temperature, the chemical potential, and the electron mass the number densities are

$$n_- = \frac{eB}{(2\pi)^2}\sum_{\eta=0}^{\infty}\int_0^\infty \mathrm{d}p \frac{1}{\exp(\sqrt{p^2+2\eta eB}/T)+1} = \frac{eBT\ln(2)}{(2\pi)^2}+\frac{2eB}{(2\pi)^2}K_2\left[\sqrt{2eB}/T\right]T, \quad (11)$$

$$n_+ = \frac{2eB}{(2\pi)^2}K_2\left[\sqrt{2eB}/T\right]T. \quad (12)$$

In Fig. 3b one can see a sizable deviation of the analytical form from the numerical result starting at $\sqrt{2eB} \sim 2T$ and until $\sqrt{2eB} \sim 7T$. The reason might be the change in the summation to an integration over the Landau levels during the calculation of the number density. A solution to this problem might be a mathematically more correct way for the transition from the sum to the integral, i.e. the Euler-MacLaurin formalism as used by Suh & Mathews (2000). In Table 1 we give a summary of all the analytic solutions for the polarisation discussed here.

3. Calculation of pulsar velocities

The specific heat capacity per volume for quark matter can be calculated from the internal energy density ϵ by

$$c_q = \left(\frac{\partial\epsilon}{\partial T}\right)_{V,N} = 9\mu^2T\left(1-\frac{2\alpha_s}{\pi}\right)+\frac{21}{5}\pi^2T^3\left(1-\frac{50\alpha_s}{21\pi}\right), \quad (13)$$

where quark interactions have been taken into account by perturbative QCD calculations to first order in the strong coupling constant $\alpha_s = g^2/(4\pi)$ (see e.g. Glendenning 2000) with the degeneracy factor $g = 2 \times 3 \times 3 = 18$. Proto neutron stars can have temperatures up to 50 MeV with quark chemical potentials in the range of (400–500) MeV. The chemical potentials for the electrons are much lower. Therefore the heat capacities for quarks c_q are much greater than the ones for the electrons and the total heat capacity is then, to a good approximation,

$$c_{\mathrm{total}} = c_q = 9{\mu_q}^2T\left(1-\frac{2\alpha_s}{\pi}\right). \quad (14)$$

As already discussed, the kick mechanism under investigation is based on anisotropically emitted neutrinos that accelerate the neutron star. The amount of acceleration depends on the polarisation of the electron spin and the neutrino momenta, respectively. Assuming a negligible neutrino mass, we can write for

the kick velocity

$$\mathrm{d}v = \frac{\chi}{M_{\rm ns}}\frac{4}{3}\pi R^3 \epsilon_{q\beta}\mathrm{d}t, \tag{15}$$

where $\epsilon_{q\beta}$ is the neutrino emissivity, R the radius of the neutrino emitting quark phase, and χ the fraction of polarised neutrinos. Using $\epsilon_{q\beta} = -\mathrm{d}\epsilon/\mathrm{d}t$ the velocity of the neutron star will depend on the energy density:

$$v = \frac{4}{3}\pi R^3 \frac{\chi}{M_{\rm ns}}(\epsilon(t_0) - \epsilon(t_{\rm f})) = \frac{4}{3}\pi R^3 \frac{\chi}{M_{\rm ns}}\Delta\epsilon \tag{16}$$

$$\sim 700\ \mathrm{km\,s^{-1}}\,\chi\left(\frac{\Delta\epsilon}{\mathrm{MeV\ fm^{-3}}}\right)\left(\frac{R}{10\ \mathrm{km}}\right)^3\left(\frac{1.4\,M_\odot}{M_{\rm ns}}\right). \tag{17}$$

In principle the difference in energy densities in Eq. (16) could be produced in various ways in quark matter, e.g. due to the transition from an ungapped to a paired quark matter phase (Drago et al. 2007; see Sect. 5) or oscillations of the magnetisation in the latter (Noronha & Shovkovy 2007). For the time being, we concentrate on $\Delta\epsilon$ originating from temperature decay. Hence,

$$v = \frac{2}{3}\pi R^3 \frac{\chi}{M_{\rm n} s} 9\left(1 - \frac{2\alpha_{\rm s}}{\pi}\right)\mu_{\rm q}{}^2 T_0^2 \tag{18}$$

$$\sim 40\ \mathrm{km\,s^{-1}}\,\chi\left(\frac{\mu_{\rm q}}{400\ \mathrm{MeV}}\right)^2\left(\frac{T_0}{\mathrm{MeV}}\right)^2\left(\frac{R}{10\ \mathrm{km}}\right)^3\frac{1.4\,M_\odot}{M_{\rm ns}}, \tag{19}$$

where T_0 is the initial temperature. From Eq. (19) we can see that the crucial input for the acceleration is the thermal energy stored in the medium. A proto-neutron star cools down to temperatures below 1 MeV during the first minutes after the supernova explosion (Lattimer & Prakash 2004). Therefore the final temperature in Eq. (19) can be neglected. For $\alpha_{\rm s} = 0.5, \mu_{\rm q} = 400$ MeV, $M_{\rm ns} = 1.4\ M_\odot$, and $\chi = 1$, the dependency of the kick velocity on the temperature and the radius of the neutrino emitting quark phase is plotted in Fig. 5. The higher the temperature of the quark phase, the higher is the neutrino energy, $E_\nu = 3.15\ T$, which results in smaller required radii R for a given velocity. For an initial temperature of $T > 5$ MeV, a kick of 1000 km s^{-1} is possible for $R < 10$ km. From Fig. 2 we find that these temperatures require magnetic fields in the range of $B \sim 10^{17}$ G to achieve full polarisation for different electron chemical potentials.

In these calculations we neglect any effects from the magnetic field on the energy density of quarks and electrons. The reader should note that the large magnetic fields might tend to lower the central density of the star (see therefore Eq. (6)) if the magnetic field is high enough to consider Landau levels but still small enough to fulfil the condition $2eB < \mu^2$; that is, the number of Landau levels is large. Considering magnetic field strengths in the range of 10^{16}–10^{17} Gauss and temperatures around 1–10 MeV, the phase space of the electrons will differ from the one of relativistic fermions. However, the electron contribution to the total energy density is very small. The quark chemical potential is between 400 to 500 MeV. According to $\eta_{\rm max} = (\mu^2 - m^2)/(2eB)$ the total number of Landau levels will be in the range of 10–1000 for magnetic fields of $B = 10^{18}$ G to $B = 10^{16}$ G.

4. Discussion of the kick velocity considering neutrino mean free paths

For hybrid stars or strange stars with a nuclear crust, we have to consider at least four neutrino interaction processes with the medium: the absorption of neutrinos in quark matter and neutron matter, as well as in the scattering processes. We will take these mean free paths from Iwamoto (1981). Nonetheless, we have to keep in mind that Iwamoto did not consider magnetic field effects and assumed degenerate electrons that will not be the case for high temperatures. For the latter one can apply the results of Burrows (1980), who arrives at a temperature dependence of the Urca emissivity of T^7 instead of the T^6 behaviour for non-degenerate electrons. More modern calculations of the neutrino mean free path in colour-flavour locked quark matter were done e.g. by Reddy et al. (2003).

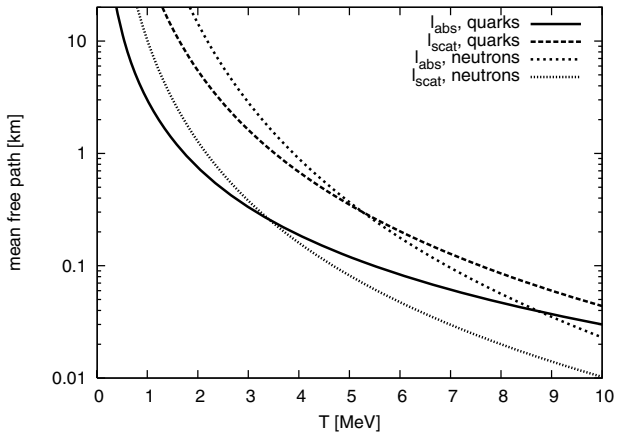

Fig. 4. Neutrino mean free paths in quark matter and neutron matter for $E_\nu = 3.15T$, $\mu_{\rm q} = 400$ MeV, $\alpha_{\rm s} = 0.5$, $n_{\rm n} = n_0$ and $\mu_{\rm e}$=10 MeV.

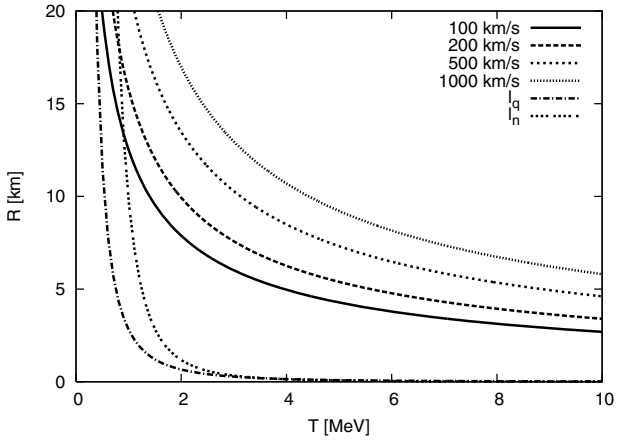

Fig. 5. Neutrino mean free paths in quark matter and neutron matter for $E_\nu = 3T$, $\mu_{\rm q} = 400$ MeV, $\alpha_{\rm s} = 0.5$, $n_{\rm n} = 0.16$ fm^{-3} and $\mu_{\rm e} = 10$ MeV with kick velocities for $M_{\rm ns} = 1.4\ M_\odot$ and full electron spin polarisation.

In Fig. 4 we plot the neutrino mean free paths as given in the Table 2 (second column) as a function of the temperature.

For subsequent discussions we combine the neutrino mean free paths for quark matter and neutron matter using

$$1/l^i_{\rm total} = 1/l^i_{\rm abs} + 1/l^i_{\rm scatt}, \tag{20}$$

with $i = n$ (neutron matter) or q (quark matter).

The radius and temperature dependence of the kick velocity, together with the total neutrino mean free paths for quark and neutron matter as calculated in Eq. (20) is plotted in Fig. 5. Different neutron star velocities for a given initial temperature T and a quark phase radius R are shown. The stars are assumed to have a total mass of 1.4 $M_\odot$. For a temperature of 5 MeV, the

Table 2. Neutrino mean free paths l for absorption and scattering processes in quark matter, as well as in neutron matter with $n_0 = 0.16$ fm^{-3} and the neutron Fermi momentum $p_{\rm Fn} = \left(3\pi^2 n_{\rm n}\right)^{1/3} \simeq 330\,(n_{\rm n}/n_0)^{1/3}$ MeV.

Process	Mean Free Path l (Iwamoto 1981)	l For $E_\nu = 3.15\,T, \alpha_{\rm s} = 0.5$ [km]	l For $T = 5$ MeV, $\mu_{\rm e} = 10$ MeV [m]
$d + \nu_e \longrightarrow u + e^-$	$\frac{1}{l^d_{\rm abs}} = \frac{4}{\pi^4}\alpha_{\rm s} G_F^2 \cos^2\Theta_c p_{\rm F}^{\rm d} p_{\rm F}^{\rm u} p_{\rm F}^{\rm e^-} \left(\frac{E_\nu^2+(\pi T)^2}{1+e^{-E_\nu/T}}\right)$	$\sim 30 \left(\frac{T}{\rm MeV}\right)^{-2} \left(\frac{\mu_{\rm q}}{400\ \rm MeV}\right)^{-2} \left(\frac{\mu_{\rm e}}{\rm MeV}\right)^{-1}$	~ 120 for $\mu_{\rm q} = 400$ MeV
$q + \nu \longrightarrow q + \nu$	$l^i_{\rm scat} = \frac{20}{C_{Vi}^2+C_{Ai}^2} \frac{1}{n_i \sigma_0} \left(\frac{m_{\rm e}}{E_\nu}\right)^2 \left(\frac{p_{\rm F}(i)}{E_\nu}\right)$	$\sim 40 \left(\frac{\mu_{\rm q}}{400\ \rm MeV}\right)^{-2} \left(\frac{T}{\rm MeV}\right)^{-3}$	~ 350 for $\mu_{\rm q} = 400$ MeV
$n + n + \nu_e \longrightarrow n + p + e^-$	$l^n_{\rm abs} = \frac{45 \rm km}{(y^4+10\pi^2 y^2+9\pi^4)} \left(\frac{T}{10\ \rm MeV}\right)^{-4} \left(\frac{n_b}{n_0}\right)^{-2/3}$	$\sim 230 \left(\frac{T}{\rm MeV}\right)^{-4} \left(\frac{p_{Fn}}{330\ \rm MeV}\right)^{-2}$	~ 370 for $n_{\rm n} = n_0$ ~ 130 for $n_{\rm n} \simeq 5n_0$
$n + \nu \longrightarrow n + \nu$	$l^n_{\rm scat} = \left(\frac{3}{32}\left(1+3g_A^2\right) n_{\rm n} \sigma_0 \left(\frac{E_\nu}{m_{\rm e}}\right)^2 \left(\frac{T}{E_F(n)}\right)\right)^{-1}$	$\sim 10 \left(\frac{T}{\rm MeV}\right)^{-3} \left(\frac{p_{Fn}}{340\ \rm MeV}\right)^{-1}$	~ 80 for $n_{\rm n} = n_0$ ~ 50 for $n_{\rm n} \simeq 5n_0$

mean free paths in neutron matter and quark matter are in the range of only 100 m, as can be seen from Table 2, and therefore up to a factor 100 smaller than the quark phase radius. For decreasing $\alpha_{\rm s}$ Eq. (14) predicts an increase in the heat capacity and consequently in the kick velocities (see Eq. (19)). The same holds for the neutrino mean free path for neutrino quark interactions as seen in Table 2 considering that $\mu_{\rm quark} = \left(1 + \frac{2\alpha_{\rm s}}{3\pi}\right) p_{F,\rm quark}$, whereas the absorption and scattering of neutrinos in hadronic matter remain unchanged. A value of $\alpha_{\rm s} \sim 0.3$ is normally expected for quark chemical potentials in the range of 1 GeV (Eidelman et al. 2004). But even for such a low value we see from Fig. 6a that the change in the neutrino mean free path in quark matter and the kick velocities is very small. From Eq. (19) we again expect an increase in the kick velocity but also a decrease in the neutrino mean free path for $\mu_{\rm q} = 500$ MeV in comparison to Fig. 5, where the quark chemical potential was set to 400 MeV. Consequently, we apply a combination of a small strong coupling constant $\alpha_{\rm s} = 0.3$ to increase the neutrino mean free path and a large quark chemical potential $\mu_{\rm q} = 500$ MeV to get higher kick velocities. The results are shown in Fig. 6c. For quark phase radii of approximately 20 km and temperatures of $\sim$0.5 MeV a kick velocity of 100 km s^{-1} is reachable. Of course such a large radius is not realistic for a quark star. Consequently neither the variation in the strong coupling constant $\alpha_{\rm s}$ nor the change of quark chemical potential will give much improvement for the final kick velocities. As can be seen in Fig. 6d, a significant change in the neutrino-quark reaction rate can be achieved by lowering the electron chemical potential. However, the original mean free paths taken from Iwamoto (1981) were calculated assuming degenerate electrons, i.e. $\mu_{\rm e} \gg T$. Consequently, for $T > \mu_{\rm e}$ the electron chemical potential in the absorption mean free path for quark matter is replaced by the temperature, as shown by Burrows (1980) for the neutrino emissivity in the direct quark Urca process. Electron-positron pair production due to the high temperature and their effects on the neutrino interaction rate have been ignored. The neutrino mean free path in quark matter hits the 100 km s^{-1} velocity curve for $R \sim 11$ km and $T \sim 1$ MeV. The 200 km s^{-1} line is reached for $R \sim 15$ km and $T \sim 1.2$ MeV. In these cases the corresponding mean free paths in neutron matter are in the range of $\sim$6 km. Hence, in this simple approximation, one can construct pulsar kicks with a velocity in the range of 100 km s^{-1} and possibly 200 km s^{-1}. The magnetic field required in this case to polarise the electrons can be taken from Fig. 2 and is in the range of $\sim 10^{16}$ Gauss. For such values of the magnetic field, the number of quark Landau levels is very high, namely in the range of 1000 assuming a quark chemical potential of 400 MeV. Consequently the influence of the magnetic field on the quark equation of state should be quite small or even negligible.

The condition $\mu_{\rm e} \ll T$ can be realised in a colour-superconducting quark phase due to the presence of strange quarks (the CFL phase does not require any electrons for charge neutrality, Rajagopal & Wilczek 2001). In unpaired strange quark matter, $\mu_{\rm e} \simeq m_{\rm s}^2/4\mu_{\rm q} \sim$ 5–6 MeV for $m_{\rm s} = 100$ MeV and $\mu_{\rm q} =$ 400–500 MeV. Strange stars have another feature that would boost the maximum possible kick velocity. The size of the hadronic phase for a hybrid star can vary between 1 and 3 km; see e.g. Schertler et al. (2000). A strange star with $M_{\rm ns} = 1.5\,M_\odot$ can have a nuclear crust of only 100–500 m thickness (Glendenning & Weber 1992). Recently, it was proposed by Jaikumar et al. (2006) that the crust of strange stars can be composed of strange quark nuggets and electrons. The thickness of such a crust is calculated to be just 50 m. The neutrino mean free path is then similar to a bare strange star, and one can ignore effects from the neutrino interactions, so that the final kick is maximal.

5. Effects of colour-superconductivity

Since it is difficult to evade the problem of the high neutrino interaction rates in hot and dense matter by varying $\alpha_{\rm s}, \mu_{\rm e}$, or $\mu_{\rm q}$, we have to look for another mechanism.

The neutrino mean free path is certainly affected by strong magnetic fields. In particular electrons are bound to Landau levels. The energy separation between two Landau levels is $\sqrt{2eB}$, which would be around 30 MeV for $B = 10^{17}$ Gauss and in the range of 10 MeV for $B = 10^{16}$ Gauss. The quantised energy levels act as a gap and suppress the neutrino quark interaction, at least in the plane perpendicular to B.

Another suppression mechanism arises in quark matter if it is in a colour-superconducting phase. If the temperature is lower than a critical temperature, pairing of quarks increases the neutrino mean free paths. To suppress neutrino quark interactions in general, all quarks have to be paired, which is the case in the CFL phase. Here charge neutrality is provided by the equal amounts of down, up, and strange quarks, which means that the presence of electrons is not required (Rajagopal & Wilczek 2001). On the other hand, electrons can be present in the system via electron-positron pair production at finite temperature. In addition, a metallic CFL (mCFL) phase with nonzero $\mu_{\rm e}$ can appear for β-stable matter for temperatures higher than $\sim$10 MeV (Rüster et al. 2004). Consequently, it would be interesting to study the neutrino emission from quark matter in the mCFL phase as it provides the quark core with significant $\mu_{\rm e}$

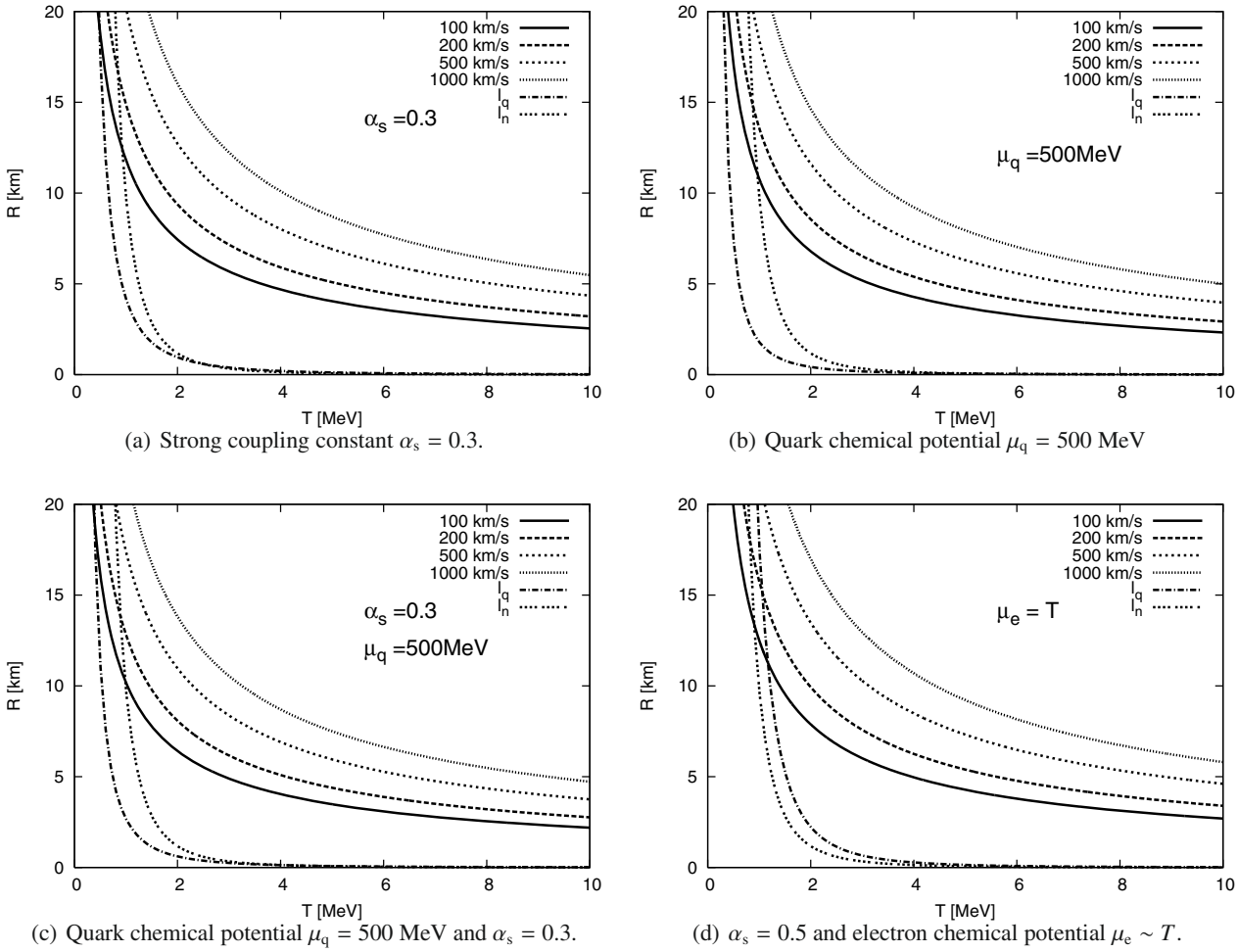

(a) Strong coupling constant $\alpha_s = 0.3$.
(b) Quark chemical potential $\mu_q = 500$ MeV
(c) Quark chemical potential $\mu_q = 500$ MeV and $\alpha_s = 0.3$.
(d) $\alpha_s = 0.5$ and electron chemical potential $\mu_e \sim T$.

Fig. 6. Kick velocities and neutrino mean free paths in quark matter and neutron matter as in Fig. 5.

(Rüster et al. 2005), as well as suppressed quark interactions. Unfortunately, the pairing between quarks decreases the quark heat capacity by $\exp(-\Delta(T)/T)$, where Δ is the gap energy (Blaschke et al. 2001). For high values of Δ, c_q is lowered drastically. Consequently, the electron heat capacity

$$c_e = \frac{{\mu_e}^2 T}{2} + \frac{7}{30} g \pi^2 T^3, \tag{21}$$

becomes significant. Implementing both heat capacities in Eq. (19) gives the following result for the kick velocity:

$$v = \frac{2}{3}\pi R^3 \frac{\chi}{M_{ns}} T^2 \left(\frac{{\mu_e}^2}{2} + \frac{7\pi^2 T^2}{60}\right)^2 + \frac{2}{3}\pi R^3 \frac{\chi}{M_{ns}} T^2 9 \left(1 - \frac{2\alpha_s}{\pi}\right) {\mu_q}^2 \exp(-\Delta/T). \tag{22}$$

As shown by Rüster et al. (2005) and Blaschke et al. (2005), high values for both the gap Δ and the electron chemical potential μ_e can arise in the colour superconducting quark core.

Since we mainly want to study the behaviour of the neutrino mean free paths and the kick size in principle, we will use the following estimates. We choose the quark chemical potential to be 450 MeV (see Rüster et al. 2005; Blaschke et al. 2005), $\mu_e =$ 100 MeV and $\Delta = 100$ MeV. The kick velocity and the mean free paths are plotted in Fig. 7 for $\alpha_s = 0.5$, $\mu_q = 450$ MeV with

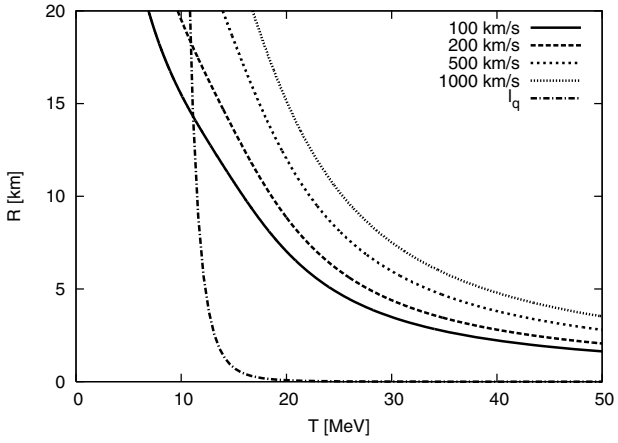

Fig. 7. Kick velocities and neutrino mean free path in quark matter for the CFL quark phase with $\alpha_s = 0.5$, $\mu_q = 450$ MeV, $\mu_e = 100$ MeV, and $\Delta = 100$ MeV.

temperatures up to 50 MeV. These values for T are of course quite high, but well in the range of proto-neutron star evolution (see e.g. Lattimer & Prakash 2004).

Comparing Figs. 5 and 7, we see the consequence of the decreased quark heat capacity. For radii $R < 10$ km, velocities of 1000 km s^{-1} can be reached for $T > 30$ MeV. For increasing

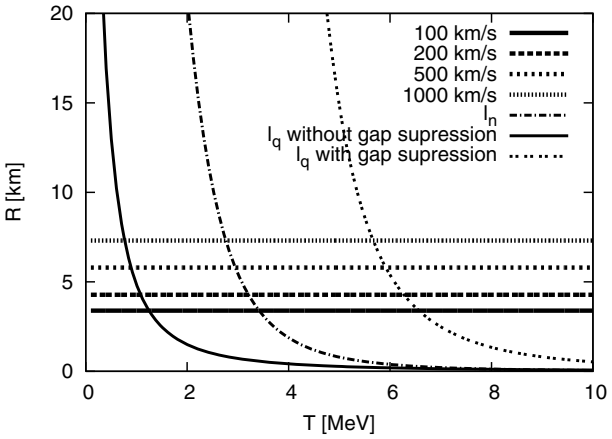

Fig. 8. Kick velocities due to a phase transition from ungapped to paired quark matter with $\mu_q = 450$ MeV and $\Delta = 20$ MeV. Neutrino mean free paths are plotted assuming an electron chemical potential of 10 MeV and normal nuclear matter density for hadronic matter. The neutrino energy is $E_\nu = \Delta^2/\mu_q$. For the quark phase, gap suppression is also taken into account (solid line). In addition, the neutrino mean free path in normal quark matter is plotted (dotted line).

temperatures the suppression factor from the gap, $\exp(-\Delta/T)$, diminishes and the contribution from quark matter becomes dominant again. As all neutrino-quark interactions are suppressed, the neutrino mean free path is greatly enhanced for $T \ll \Delta$. However, the kick velocity is reduced at high temperatures so that just the values for $v < 100\,\mathrm{km\,s^{-1}}$ can be reached for free streaming neutrinos and realistic quark phase radii. As can be seen from Fig. 7, a quark phase radius of ∼14 km is required to accelerate the star to $100\,\mathrm{km\,s^{-1}}$.

Regarding the high temperatures and the high electron chemical potential discussed here, the magnetic fields for fully polarised electrons are expected to be extremely high. For $T > 10$ MeV and electron chemical potentials of $\mu_e > 80$ MeV, the magnetic fields must be stronger than 10^{18} G and therefore higher than the critical value of $\sim 1.3 \times 10^{18}$ Gauss for stability (Lai & Shapiro 1991). Reddy et al. (2003) calculated neutrino mean free paths in the colour-flavour locked phase to be larger than 10 km for a temperature of $T = 5$ MeV. However, they find that the interaction with massless bosons, which appear due to the breaking of baryon number conservation in the CFL phase, leads to a mean free path that is similar to or even shorter than the one for normal quark matter. For temperatures of around 30 MeV, this means a very low value for the mean free path in the range of cm, which would make the acceleration mechanism even in gapped quark matter unfeasible.

From Eq. (16) we know that a high kick velocity requires a sufficient energy release. Up to now, the neutrino energy was given by the temperature. In the case of a phase transition from an unpaired to a gapped quark matter phase with the gap Δ, an energy of $3\Delta^2\mu_q^2/\pi^2$ would be released (Alford et al. 2001). If we assumed a neutrino emission of one neutrino per quark, the energy per neutrino would be Δ^2/μ_q. For the case $\Delta^2/\mu_q \sim 1$ MeV the gap would be in the range of 20 MeV for $\mu_q \sim 450$ MeV. Consequently, for low temperatures, the neutrino mean free path would be large as seen in Table 2. At the same time the energy release $3\Delta^2\mu_q^2/\pi^2 \sim 3.2\,\mathrm{MeV/fm^3}$ would be strong enough to accelerate the star to $1000\,\mathrm{km\,s^{-1}}$ if the quark phase radius was in the range of 7 km (see Eq. (17)). This scenario is plotted in Fig. 8 where the energy release is assumed to be completely emitted by neutrinos accelerating the compact star.

Considering gap suppression of the neutrino quark interactions, we get kick velocities of $1000\,\mathrm{km\,s^{-1}}$ for a quark phase radius in the range of 7 km and a temperature less than 6 MeV. However, to accommodate for the interaction with the massless H boson in the CFL phase, we plot the neutrino mean free path in normal quark matter and get allowed temperatures in the range of <1 MeV. For these values for the temperature and an electron chemical potential in the range of 10 MeV, the magnetic fields that are required to fully spin polarise the electrons are in the range of 10^{16} G.

However, in a more realistic scenario, the energy release will not be entirely transferred to neutrinos but will also go into photons as well as heat. As a consequence the neutrino energy will be lower, which requires a larger quark phase. Also the neutrino mean free path will decrease due to the higher temperature that most probably will make it difficult to reach high velocities. In this connection it is interesting to study a scenario proposed by Drago et al. (2007), where the authors discuss the transformation of a hadronic star into a quark star or a hybrid star. They find the formation of a convective layer in the case of conversion from ungapped (e.g. 2SC) to gapped quark (CFL) matter. An asymmetry in the fast transport of hot CFL quark matter to the surface of the hybrid or quark star might be able to create large kicks.

6. Summary and outlook

In this work we critically studied an acceleration mechanism for pulsars based on asymmetric neutrino emission from the direct quark Urca process in the interior of magnetised proto neutron stars. The neutrinos are created in the direct quark Urca process by the cooling strange quark matter core of the compact star with their energy given by $3.15\,T$. The neutrino anisotropy arises due to a strong magnetic field that forces the electrons into the lowest Landau level where their spin is polarised opposite to the magnetic field direction. To fully spin polarise the electrons for initial temperatures of 1–10 MeV, we find the required magnetic field strength to be about 10^{16}–10^{18} Gauss, depending on the electron chemical potential. The pulsar kick velocity depends on the released energy in the quark phase and in our case stems from the heat reservoir.

For fully spin polarised electrons, we find that a kick velocity of $1000\,\mathrm{km\,s^{-1}}$ is possible for an initial temperature of $T > 5$ MeV, a radius of $R < 10$ km, and the mass of $1.4\,M_\odot$ suitable for a strange star. The required magnetic fields have to be in the range of $B \sim 10^{17}$ G to achieve full polarisation for electron chemical potentials of $\mu_e < 30$ MeV.

However, as shown by Kusenko et al. (1998) high neutrino quark interaction rates will wash out the beamed flux of neutrinos necessary for the acceleration mechanism. For typical properties of quark matter in the interior of a quark star, the neutrino mean free paths range between 100 m and 800 m (Iwamoto 1981) which is too small, at least for the quark matter core. The best results were found for $\alpha_s = 0.5$, $\mu_q = 400$ MeV and $\mu_e \sim T$, giving a velocity of $100\,\mathrm{km\,s^{-1}}$ for quark phase radii of $R \sim 11$ km and a temperature in the range of $T \sim 1$ MeV. A kick velocity of $200\,\mathrm{km\,s^{-1}}$ was reached for $R \sim 15$ km and $T \sim 1.2$ MeV. For both cases the required magnetic field is in the range of $\sim 10^{16}$ Gauss.

The presence of the colour-flavour locked quark matter phase (CFL) will suppress the neutrino quark interactions and provide a small electron chemical potential. In this case the neutrino mean free path is enlarged by a factor $\exp(\Delta/T)$ where Δ is the pairing energy of the quarks. However, the quark heat capacity

also decreases exponentially with Δ/T so that the highest reachable kick velocity is again 100 km s^{-1} for a gap of $\Delta = 100$ MeV, $\mu_e = 100$ MeV, a quark chemical potential $\mu_q = 450$ MeV, and a quark phase radius of $R = 14$ km. For such high values of μ_e, the magnetic fields for full polarisation are larger than the critical value of $\sim 1.3 \times 10^{18}$ Gauss for stability (Lai & Shapiro 1991).

Consequently, the mechanism discussed here can produce neutron star velocities of 1000 km s^{-1} only if neutrino quark interactions can be ignored. Otherwise asymmetric neutrino emission from paired and unpaired quark matter fail to describe pulsar kicks due to the small neutrino mean free paths. The latter effect seems to make it impossible to reach velocities higher than 100 km s^{-1}. For the neutrino mean free path to be large, small temperatures are required. At the same time, the energy release should be large to accelerate the compact star to high velocities.

An interesting mechanism might be a phase transition from unpaired to gapped quark matter as discussed by e.g. Drago et al. (2007), where the energy release is about $3\Delta^2\mu_q^2/\pi^2$ and could accelerate the neutron star to 1000 km s^{-1} assuming $\mu_q \sim 450$ MeV and $\Delta \sim 20$ MeV. The energy carried off by neutrinos would be $\sim \Delta^2/\mu_q$ per neutrino, which is in the range of 1 MeV and therefore small. Velocities of 1000 km s^{-1} can be reached for temperatures up to around 6 MeV only when including the suppression of the neutrino quark interaction by the pairing gap. If we neglect the gap suppression to compensate for the interaction with the massless H boson in the CFL phase the allowed temperatures decrease to <1 MeV. For such temperatures and electron chemical potentials around 10 MeV, the required magnetic field to fully spin-polarise electrons is in the range of 10^{16} G. In a more realistic approach, effects from quark pairing in the CFL phase and magnetic field for the heat capacities and particle energy densities have to be included. It should also be considered that the energy release will not be entirely transferred to neutrinos but will also go into photons and heat, which will lower the neutrino energy requiring a larger quark phase radius. The energy release in neutrinos and therefore the kick velocities and the neutrino mean free path in the neutron star's interior needs to be studied in more detail.

In this work we did not include the influence of the magnetic field on either the equation of state for the electrons or on the one for the quarks. A strong magnetic field might tend to lower the central density of the star and therefore inhibit the formation of quark matter.

The consequence of our analysis is a pessimistic result for the pulsar kicks caused by asymmetric neutrino emission from quark matter in the interior of cooling proto neutron stars. Both unpaired and paired strange quark matter fail to describe pulsar kicks. Also for the neutrinos stemming from a phase transition to colour superconducting quark matter, high kick velocities are difficult to reach due to small neutrino mean free paths. However, for low temperatures there are situations where our analysis does not exclude high velocities. The evolution of a proto neutron star has to be studied in a full dynamical treatment before final conclusions about the kick mechanism due to quark matter can be drawn.

Acknowledgements. I. Sagert is supported by the Helmholtz Research School for Quark Matter studies in Heavy Ion Collisions.

References

Alford, M. 2001, Ann. Rev. Nucl. Part. Sci., 51, 131
Alford, M., Rajagopal, K., & Wilczek, F. 1998, Phys. Lett. B, 422, 247
Alford, M., Rajagopal, K., & Wilczek, F. 1999, Nucl. Phys. B, 537, 443
Alford, M., Rajagopal, K., Reddy, S., & Wilczek, F. 2001, Phys. Rev. D, 64, 074017
Alford, M., Blaschke, D., Drago, A., et al. 2007, Nature, 445, 7
Arzoumanian, Z., Chernoff, D. F., & Cordes, J. M. 2002, ApJ, 568, 289
Bailin, D., & Love, A. 1984, Phys. Rep., 107, 325
Barrois, B. C. 1977, Nucl. Phys. B, 129, 390
Berdermann, J., Blaschke, D., Grigorian, H., & Voskresensky, D. N. 2006, Prog. Part. Nuc. Phys., 57, 334
Blaschke, D., Grigorian, H., & Voskresensky, D. N. 2001, A&A, 368, 561
Blaschke, D., Fredriksson, S., Grigorian, H., Öztaş, A. M., & Sandin, F. 2005, Phys. Rev. D, 72, 065020
Bombaci, I., & Popov, S. B. 2004, A&A, 424, 627
Brisken, W. F., Romani, R. W., & Ng, C. Y. 2005, in X-Ray and Radio Connections, http://www.aoc.nrao.edu/events/xraydio, ed. L. O. Sjouwerman, & K. K. Dyer
Burrows, A. 1980, Phys. Rev. Lett., 44, 1640
Burrows, A., Livne, E., Dessart, L., Ott, C. D., & Murphy, J. 2006, ApJ, 640, 878
Byckling, E., & Kajantie, K. 1973, Particle Kinematics (New York: John Wiley & Sons)
Chatterjee, S., Vlemmings, W. H. T., Brisken, W. F., et al. 2005, ApJ, 630, L61
Cordes, J. M., & Chernoff, D. F. 1998, ApJ, 505, 315
Dorofeev, O. F., Rodionov, V. N., & Ternov, I. M. 1985, SvA Lett., 11, 123
Drago, A., Lavagno, A., & Pagliara, G. 2004, J. Phys. A, 19, 197
Drago, A., Lavagno, A., & Parenti, I. 2007, ApJ, 659, 1519
Eidelman, S., Hayes, K., Olive, K., et al. 2004, Phys. Lett. B, 592, 1
Glendenning, N. K. 1992, Phys. Rev. D, 46, 1274
Glendenning, N. K. 2000, Compact Stars – Nuclear Physics, Particle Physics, and General Relativity, 2nd edn. (New York: Springer)
Glendenning, N. K., & Weber, F. 1992, ApJ, 400, 647
Glendenning, N. K., & Kettner, C. 2000, A&A, 353, L9
Gott, J. R. I., Gunn, J. E., & Ostriker, J. P. 1970, ApJ, 160, L91
Harrison, E. R., & Tademaru, E. 1975, ApJ, 201, 447
Hobbs, G., Lorimer, D., Lyne, A., & Kramer, M. 2005, MNRAS, 360, 974
Horowitz, C. J., & Li, G. 1998, Phys. Rev. Lett., 80, 3694
Horowitz, C. J., & Piekarewicz, J. 1998, Nucl. Phys. A, 640, 281
Huang, M. 2005, Int. J. Mod. Phys. E, 14, 675
Itoh, N. 1970, Prog. Theor. Phys., 44, 291
Iwamoto, N. 1981, Ann. Phys. (N.Y.), 141, 1
Jaikumar, P., Reddy, S., & Steiner, A. W. 2006, Phys. Rev. Lett., 96, 041101
Janka, H.-T., Marek, A., & Kitaura, F.-S. 2007, in Supernova 1987A: 20 Years After: Supernovae and Gamma-Ray Bursters, ed. S. Immler & R. McCray, Am. Inst. Phys. Conf. Ser., 937, 144
Johnston, S., Hobbs, G., Vigeland, S., et al. 2005, MNRAS, 364, 1397
Kusenko, A., Segrè, G., & Vilenkin, A. 1998, Phys. Lett. B, 437, 359
Lai, D., & Shapiro, S. L. 1991, ApJ, 383, 745 1309
Lai, D., Chernoff, D. F., & Cordes, J. M. 2001, ApJ, 549, 1111
Lattimer, J. M., & Prakash, M. 2004, Science, 304, 536
Ng, C.-Y., & Romani, R. W. 2004, ApJ, 601, 479
Ng, C.-Y., & Romani, R. W. 2007, ApJ, 660, 1357
Noronha, J. L., & Shovkovy, I. A. 2007, Phys. Rev. D, 76, 105030
Pagliara, G., & Schaffner-Bielich, J. 2008, Phys. Rev. D, 77, 063004
Rajagopal, K., & Wilczek, F. 2000, in At the Frontier of Particle Physics Handbook of QCD, ed. M. Shifman (World Scientific), 2061
Rajagopal, K., & Wilczek, F. 2001, Phys. Rev. Lett., 86, 3492
Rapp, R., Schäfer, T., Shuryak, E., & Velkovsky, M. 1998, Phys. Rev. Lett., 81, 53
Rapp, R., Schäfer, T., Shuryak, E. V., & Velkovsky, M. 2000, Ann. Phys. (N.Y.), 280, 35
Reddy, S., Sadzikowski, M., & Tachibana, M. 2003, Nucl. Phys. A, 721, 309
Rischke, D. H. 2004, Prog. Part. Nuc. Phys., 52, 197
Rüster, S. B., Shovkovy, I. A., & Rischke, D. H. 2004, Nucl. Phys. A, 743, 127
Rüster, S. B., Werth, V., Buballa, M., Shovkovy, I. A., & Rischke, D. H. 2005, Phys. Rev. D, 72, 034004
Sandin, F., & Blaschke, D. 2007, Phys. Rev. D, 75, 125013
Schaffner-Bielich, J. 2005, J. Phys. G, 31, 651
Schaffner-Bielich, J. 2007, in MPE report, 291, 363, Heraeus Seminar on Neutron Stars and Pulsars: 40 Years After the Discovery, ed. W. Becker & H. Huang, 181
Schertler, K., Greiner, C., Schaffner-Bielich, J., & Thoma, M. H. 2000, Nucl. Phys. A, 677, 463
Schmitt, A., Shovkovy, I. A., & Wang, Q. 2005, Phys. Lett., 94, 211101
Shovkovy, I. A. 2005, Found. Phys., 35, 1309
Shul'man, G. A. 2001, Russ. Phys. J., 44, 90
Suh, I.-S., & Mathews, G. J. 2000, ApJ, 530, 949
Wang, C., Lai, D., & Han, J. L. 2006, ApJ, 639, 1007
Weber, F. 2005, Prog. Part. Nuc. Phys., 54, 193